Numerical Simulation of Nonlinear Ultrasonic Wave Generation by an Interface Crack of Bi-material

***T. Maruyama[1], T. Saitoh[2], and S. Hirose[1]**

[1]Department of Mechanical & Environmental Informatics, Tokyo Institute of Technology
Ookayama 2-12-1, Meguro-ku, Tokyo 152-8552, Japan
[2]Division of Environmental Engineering Science, Gunma University Tenjin 1-5-1, Kiryu, Gunma 376-8515, Japan

*Corresponding author: maruyama.t.ag@m.titech.ac.jp

Abstract

Nonlinear ultrasonic nondestructive testing using contact acoustic nonlinearity has been developed over the last decade. However, although nonlinear waves such as higher- and sub-harmonics are considered to be generated by the interaction of the crack faces such as clapping motion or friction, the mechanism of generation has not been understood clearly from theoretical view point yet. 1-D and 2-D numerical simulations have been conducted, and 3-D axisymmetric problems have been numerically solved so far. However, no full 3-D analysis has been done. Therefore, in this research, the boundary integral equation for an interface crack with nonlinear boundary conditions in 3-D medium is formulated, and solved numerically using a time-domain boundary element method. The Fourier spectra of received waves are evaluated in the form of far-field scattered waves because the received points are usually located far from the defects in NDT.

Keywords: Time-domain BEM, 3-D nonlinear ultrasonic simulation, Nondestructive testing (NDT), Higher-harmonics, Sub-harmonics, Contact acoustic nonlinearity

Introduction

The nonlinear nondestructive testing (NNDT) using contact acoustic nonlinearity (CAN) is considered as one of the effective methods for the evaluation of closed cracks in metal or on interface of bi-material. Thus, some NNDT methods using CAN have been developed in order to detect cracks and measure the length of closed part of a crack [Ohara at el. (2011)]. The generation of nonlinear ultrasonic waves by the CAN was advocated over thirty years ago [Buck at el. (1978)]. At this stage, higher-harmonics were considered to be generated by the interaction of the crack faces such as clapping motions or friction due to large amplitudes of incident waves [Solodov at el. (2011)]. However, the generation mechanism of sub-harmonics has not been understood clearly yet. Therefore, it is needed to investigate the mechanism more from the theoretical or numerical point of view.

In previous researches, 2-D numerical simulations were carried out [Hirose (1994); Saitoh at el. (2011)]. 3-D axisymmetric problem of a penny-shaped crack subjected to normal incidence of a longitudinal wave was solved numerically [Hirose at el. (1993)]. However, no full 3-D analysis has been done. Therefore, in this research, the 3-D boundary integral equation (BIE) is formulated for an interface crack of bi-material with nonlinear boundary conditions and numerically solved using the time-domain boundary element method (BEM) in order to investigate the relation between the analysis conditions, such as frequencies of an incident wave and size of a crack, and the generation of higher- and sub-harmonics.

In the proposed numerical method, the implicit Runge-Kutta (IRK) based convolution quadrature method (CQM) [Maruyama at el. (2013)] is applied to discretization of convolution integrals in BIE. Application of CQM to the discretization improves numerical accuracy and stability behavior of the time-marching process of time-domain BEM. In addition, far-field scattered waves are evaluated as received waves and used for the Fourier spectrum analysis because the received points are usually located far from the defects compared with the defect size and wave length in NDT.

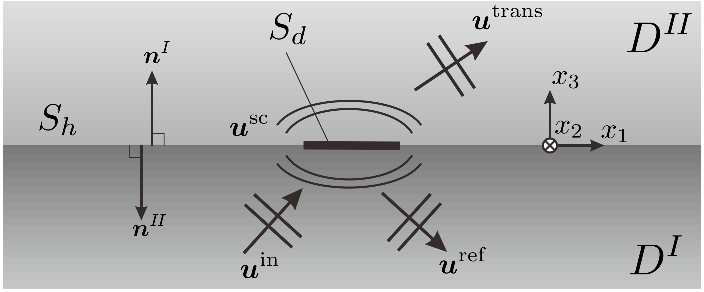

Figure 1. Debonding area of bi-material interface subjected to an incident plane wave.

Formulation of boundary integral equations

A 3-D boundary element analysis model for nonlinear ultrasonic simulation is considered for two-layer problems including the debonding area as shown in Fig. 1. This model consists of two semi-infinite domains, D^I and D^{II} , and the interfaces between them, S_h and S_d, denote bonding and debonding areas, respectively. In addition, $\boldsymbol{n}^I$ and $\boldsymbol{n}^{II}$ are defined as unit vectors pointing into outer normal directions from respective domains where the upper subscripts, I and II, indicate the respective domains. In this analysis, a plane wave is used as the incident wave to investigate fundamental motions of the nonlinear crack.

For the layered problems subjected to an incident plane wave, the free field formulation is usually used in BEM. Assuming that the interface S_h is flat, the free field $\boldsymbol{u}^{\mathrm{free}}$ which consists of incident wave $\boldsymbol{u}^{\mathrm{in}}$, reflected wave $\boldsymbol{u}^{\mathrm{ref}}$, and transmitted wave $\boldsymbol{u}^{\mathrm{trans}}$ can be calculated analytically. The scattered wave $\boldsymbol{u}^{\mathrm{sc}}$ is defined as the disturbance of $\boldsymbol{u}^{\mathrm{free}}$ by the debonding area S_d, and following equations are obtained:

$$\boldsymbol{u}^{\mathrm{free};\,I} = \boldsymbol{u}^{\mathrm{in};\,I} + \boldsymbol{u}^{\mathrm{ref};\,I}, \qquad \boldsymbol{u}^{\mathrm{free};\,II} = \boldsymbol{u}^{\mathrm{trans};\,II}, \qquad \boldsymbol{u} = \boldsymbol{u}^{\mathrm{free}} + \boldsymbol{u}^{\mathrm{sc}}, \tag{1}$$

where $\boldsymbol{u}$ is the total wave. Since $\boldsymbol{u}^{\mathrm{sc}}$ satisfies the radiation condition, the BIE is formulated for $\boldsymbol{u}^{\mathrm{sc}}$ as follows:

$$\begin{aligned}\frac{1}{2}\boldsymbol{u}^{\mathrm{sc};I(II)}(\boldsymbol{x},t) = &\int_0^t \int_{S_h+S_d} \boldsymbol{U}^{I(II)}(\boldsymbol{x},\boldsymbol{y},t-\tau)\boldsymbol{t}^{\mathrm{sc};I(II)}(\boldsymbol{y},\tau)dS_y\,d\tau \\ &- \int_0^t \mathrm{p.v.}\int_{S_h+S_d} \boldsymbol{T}^{I(II)}(\boldsymbol{x},\boldsymbol{y},t-\tau)\boldsymbol{u}^{\mathrm{sc};I(II)}(\boldsymbol{y},\tau)dS_y\,d\tau,\end{aligned} \tag{2}$$

where $\boldsymbol{t}$ is the traction force, and $\boldsymbol{U}$ and $\boldsymbol{T}$ are the fundamental solutions for displacement and traction, respectively in 3-D elastodynamics. The symbol $\mathrm{p.v.}$ indicates the Cauchy's principle integral. Substituting Eq. (1c) into Eq. (2), the BIE is expressed by $\boldsymbol{u}$ and $\boldsymbol{u}^{\mathrm{free}}$ and can be numerically solved using discretization methods for time and space and appropriate interface conditions on S_h and S_d. In addition, S_h is truncated by finite area in numerical analysis.

Discretization of BIE using IRK based CQM

In solving the BIE (2) numerically, the convolution integrals are evaluated by means of the IRK based CQM [Lubich et al. 1993] and the surface integrals over S_h and S_d are discretized by the piecewise constant boundary elements. If the m-stage Radau IIA method, which is one of the IRK methods, is used in the IRK based CQM, and the interface including the debonding area is divided into M boundary elements, the discretized BIE at the n-step and the i-sub-step in time are shown as follows:

$$\frac{1}{2}\boldsymbol{u}_{\gamma}^{I(II)}\left((n+c_i)\Delta t\right)=\frac{1}{2}\boldsymbol{u}_{\gamma}^{\text{free};I(II)}\left((n+c_i)\Delta t\right)$$
$$+\sum_{k=0}^{n}\sum_{\alpha=1}^{M}\sum_{j=1}^{m}\left[\boldsymbol{A}_{\gamma\alpha}^{ij;n-k}\left\{\boldsymbol{t}_{\alpha}^{I(II)}\left((k+c_j)\Delta t\right)-\boldsymbol{t}_{\alpha}^{\text{free};\,I(II)}\left((k+c_j)\Delta t\right)\right\}\right. \tag{3}$$
$$\left.-\boldsymbol{B}_{\gamma\alpha}^{ij;n-k}\left\{\boldsymbol{u}_{\alpha}^{I(II)}\left((k+c_j)\Delta t\right)-\boldsymbol{u}_{\alpha}^{\text{free};\,I(II)}\left((k+c_j)\Delta t\right)\right\}\right],$$

where subscripts, α and γ, are the indexes of boundary elements and c_i is the parameter in IRK method corresponding to the sub-step. In addition, $\boldsymbol{A}_{\gamma\alpha}^{ij;\kappa}$ and $\boldsymbol{B}_{\gamma\alpha}^{ij;\kappa}$ are influence functions expressed as follows:

$$\boldsymbol{A}_{\gamma\alpha}^{ij;\kappa}=\frac{\mathcal{R}^{-\kappa}}{L}\sum_{l=0}^{L-1}\left[\sum_{\beta=1}^{m}\left\{\boldsymbol{E}_{\beta}(z_l)\right\}_{ij}\int_{S_\alpha}\widehat{\boldsymbol{U}}^{I(II)}\left(\boldsymbol{x}_{\gamma},\boldsymbol{y},\lambda_{\beta}^{l}\right)dS_y\right]\mathrm{e}^{-\frac{2\pi\mathrm{i}\kappa l}{L}}, \tag{4}$$

$$\boldsymbol{B}_{\gamma\alpha}^{ij;\kappa}=\frac{\mathcal{R}^{-\kappa}}{L}\sum_{l=0}^{L-1}\left[\sum_{\beta=1}^{m}\left\{\boldsymbol{E}_{\beta}(z_l)\right\}_{ij}\,\mathrm{p.v.}\int_{S_\alpha}\widehat{\boldsymbol{T}}^{I(II)}\left(\boldsymbol{x}_{\gamma},\boldsymbol{y},\lambda_{\beta}^{l}\right)dS_y\right]\mathrm{e}^{-\frac{2\pi\mathrm{i}\kappa l}{L}}, \tag{5}$$

where ($\hat{\ }$) indicates the function in the Laplace-domain, i is the imaginary unit, and the last arguments λ_{β}^{l} of $\widehat{\boldsymbol{U}}$ and $\widehat{\boldsymbol{T}}$ correspond to Laplace parameters. In Eqs. (4) and (5), $\lambda_{\beta}^{l},\mathcal{R},L,z_l,$ and $\boldsymbol{E}_{\beta}$ are the parameters of IRK based CQM [Maruyama et al. (2013)]. The matrix-vector products on the right side of Eq. (3) are effectively calculated by means of the fast multipole method (FMM), which is one of the acceleration methods for BEM.

Nonlinear interface conditions

The interface condition on the bonding area S_h is the continuity of displacement and traction as

$$\boldsymbol{u}^{I}=\boldsymbol{u}^{II},\qquad \boldsymbol{t}^{I}=-\boldsymbol{t}^{II}. \tag{6}$$

For the debonding area S_d, three types of interface conditions, “separation”, “stick”, and “slip”, are considered [Hirose (1994); Saitoh at el. (2011)]. “separation” means that two surfaces of upper and lower materials are separated with no traction, while “stick” and “slip” are contact conditions under compressive normal stress state. For the “stick” condition, the surfaces of two materials move with no relative velocity. On the other hand, the “slip” condition allows a relative tangential movement with dynamic friction force. Therefore, these three conditions are described as follows:

$$\boldsymbol{t}^{I}=\boldsymbol{t}^{II}=\boldsymbol{0}\qquad :\ \text{separation}, \tag{7}$$

$$[u_3]=0,\qquad \boldsymbol{t}^{I}=-\boldsymbol{t}^{II},\qquad [\dot{\boldsymbol{u}}_t]=\boldsymbol{0}\qquad :\ \text{stick}, \tag{8}$$

$$[u_3]=0,\qquad t_3^{I}=-t_3^{II},\qquad \boldsymbol{t}_t^{I}=-\boldsymbol{t}_t^{II}=\frac{[\dot{\boldsymbol{u}}_t]}{\left|[\dot{\boldsymbol{u}}_t]\right|}\mu_d(-t_3^{I})\qquad :\ \text{slip}, \tag{9}$$

where $[\boldsymbol{u}]$ is the crack opening displacement and expressed by $[\boldsymbol{u}]=\boldsymbol{u}^{II}-\boldsymbol{u}^{I}$, ($\dot{\ }$) indicates the time differentiation, and the subscript t means tangential components in x_1 and x_2 directions. In addition, μ_d is the dynamic friction coefficient.

Numerical procedure

The numerical algorithm is shown in Fig. 2. At the beginning of a time step in the IRK based CQM, the discretized BIE (3) is solved assuming that the interface conditions on each element are the same as those in the previous time step. If the additional constraint conditions enclosed by the double

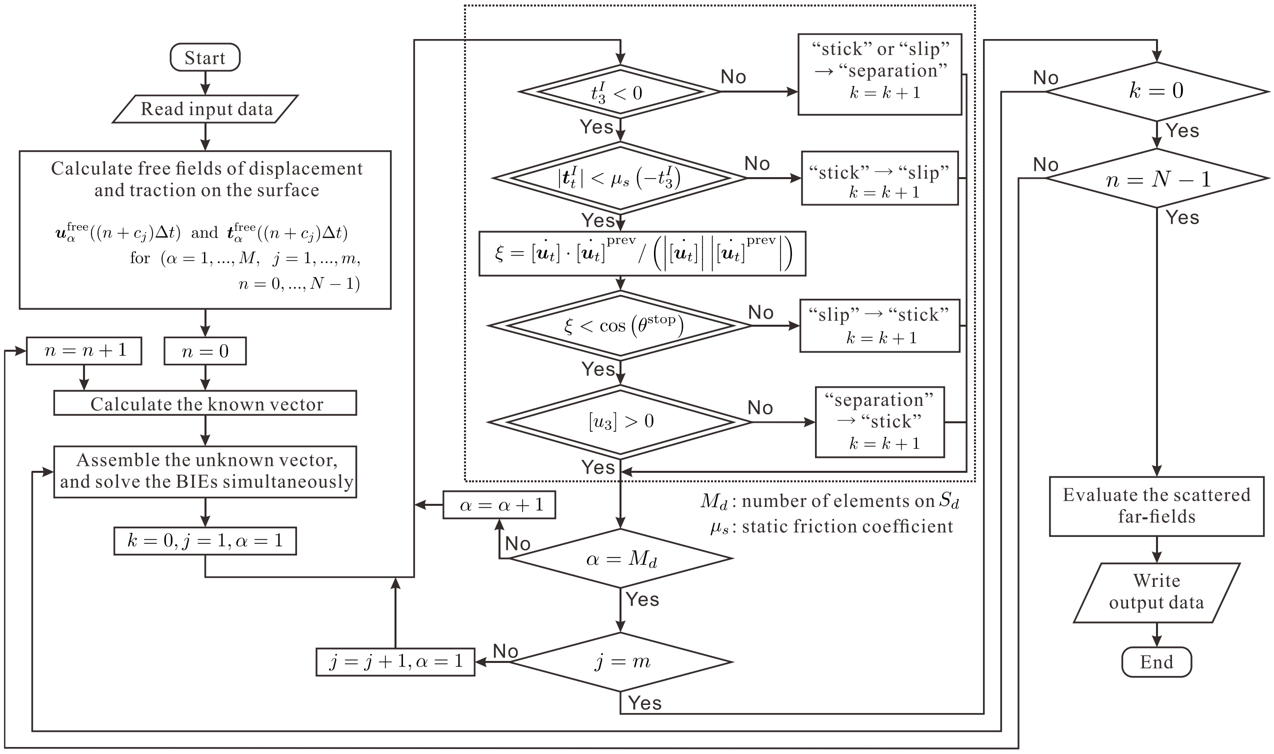

Figure 2. Numerical algorithm.

rhombuses in Fig. 2 are not satisfied, the interface condition on the element, which is one of "separation", "stick", and "slip", is changed into one of the other conditions and then the system of equations is assembled and solved again. After conducting the iterative calculations, if both the interface conditions and the additional constraint conditions on all elements at all sub-steps are satisfied, the time step proceeds to the next one.

Some remarks concerning the numerical calculations are given below. At the initial time step, the interface condition of "stick" is given on all elements on the debonding area assuming that the interface is closed before the wave incidence. There are two possible phase shifts from "separation" to one of two contact conditions, i.e., "slip" and "stick". In the present study, the priority is given to the change from "separation" to "stick", if $[u_3] > 0$ for the "separation" is violated on the element. In numerical calculations, it is difficult to achieve the condition $[\dot{\boldsymbol{u}}_t] = \boldsymbol{0}$ exactly in the transition from "stick" to "slip". Therefore, we set $[\dot{\boldsymbol{u}}_t] = \boldsymbol{0}$ unless the following condition is satisfied:

$$\xi < \cos(\theta^{\rm stop}), \qquad \xi = [\dot{\boldsymbol{u}}_t] \cdot [\dot{\boldsymbol{u}}_t]^{\rm prev} / \left(|[\dot{\boldsymbol{u}}_t]| |[\dot{\boldsymbol{u}}_t]^{\rm prev}| \right), \tag{10}$$

where $[\boldsymbol{u}]^{\rm prev}$ is the crack opening displacement at the previous time step. Eq. (10) means that the transition from "slip" to "stick" occurs when there is a big change in the slip direction. In this study, $\theta^{\rm stop}$ is given by 90 degrees.

Far-field scattered wave

In this research, the scattered wave by an interface crack at far-field [Hirose at el. (1989)] is calculated to investigate the generation of nonlinear ultrasonic waves. For example, when $\boldsymbol{x}$ is the receiver point and $\boldsymbol{y}$ is the point on a crack, the far-field scattered L wave by an interface crack of bi-material $u_L^{{\rm sc,far};I(II)}$ is given by

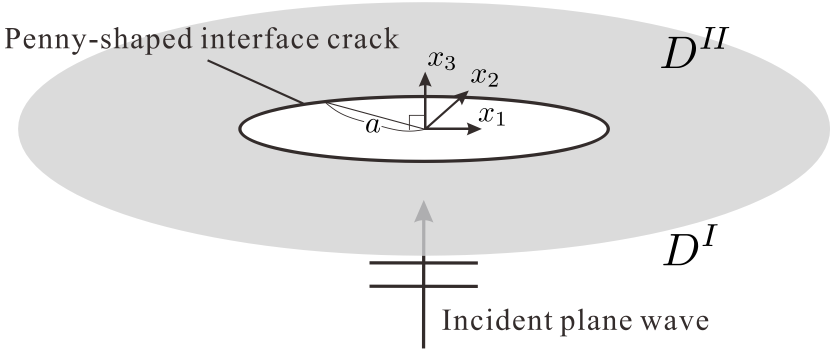

Figure 3. Scattering of an incident plane wave by a penny-shaped interface crack of bi-material.

$$u_L^{\text{sc,far};I(II)}(\boldsymbol{x},t) \simeq \frac{1}{4\pi x}\Omega_L\left(\hat{\boldsymbol{x}}, t - \frac{x}{c_L^{I(II)}}\right), \tag{11}$$

where $x = |\boldsymbol{x}|$ and $\hat{\boldsymbol{x}} = \boldsymbol{x}/x$. Ω_L is the far-field amplitude of L wave, which is expressed for $y_3 = 0$ as follows:

$$\begin{aligned}\Omega_L\left(\hat{\boldsymbol{x}}, t - \frac{x}{c_L^{I(II)}}\right) = \sum_{\alpha=L,TV} \frac{C_{pjkq}^{II(I)}}{\mu^{II(I)}} A_k^{\pm\alpha} \frac{\zeta_q^{\pm}}{c_L^{I(II)}} T^{\alpha,L}(\boldsymbol{\zeta}^{\pm}) \frac{|\hat{x}_3|}{\nu} \\ \times \int_{S_d} n_j^I(\boldsymbol{y})\,[\dot{u_p}]\left(\boldsymbol{y}, t - \left[\frac{x}{c_L^{I(II)}} - \frac{\boldsymbol{\zeta}^{\pm}\cdot\boldsymbol{y}}{c_\alpha^{II(I)}}\right]\right) dS_y\,,\end{aligned} \tag{12}$$

where C_{ijkl} is the elastic constant tensor and μ is the shear modulus. $T^{\alpha,L}(\boldsymbol{\zeta}^{\pm})$ is the transmission coefficient with incident wave propagation vector $\boldsymbol{\zeta}^{\pm}$ into $x_3 = 0$ plane when the wave mode is changed from α to L and the wave is propagating from $D^{II(I)}$ to $D^{I(II)}$. In addition, $\boldsymbol{\zeta}^{\pm}$, ν, and $A_k^{\pm\alpha}$ are given by

$$\boldsymbol{\zeta}^{\pm} = \left(\frac{c_\alpha^{II(I)}}{c_L^{I(II)}}\,\hat{x}_1, \frac{c_\alpha^{II(I)}}{c_L^{I(II)}}\,\hat{x}_2, \pm\nu\right), \qquad \nu = \sqrt{1 - \left(\frac{c_\alpha^{II(I)}}{c_L^{I(II)}}\,\hat{x}_1\right)^2 - \left(\frac{c_\alpha^{II(I)}}{c_L^{I(II)}}\,\hat{x}_2\right)^2}, \tag{13}$$

$$A_k^{\pm L} = \left(\frac{c_T^{II(I)}}{c_L^{II(I)}}\right)^2 \zeta_k^{\pm}, \qquad \boldsymbol{A}^{\pm TV} = \hat{\boldsymbol{d}}^{TH} \times \boldsymbol{\zeta}^{\pm}. \tag{14}$$

In Eq. (14), $\hat{\boldsymbol{d}}^{TH}$ is the displacement vector of the TH wave propagating to $\boldsymbol{\zeta}^{\pm}$ direction. In Eqs. (12)-(14), $\pm$ is decided by the positional relation between $\boldsymbol{x}$ and $\boldsymbol{y}$ in derivation of the Green's function, and $+$ and – correspond to $x_3 > y_3$ and $x_3 < y_3$, respectively [Achenbach at el. (1982)]. In addition, the TV and TH wave components of the far-field scattered waves are described by analogous formulas. In this study, Ω_L is used for the Fourier spectrum analysis, because the far-field scattered waves do not include the truncated error of S_h if only $[\dot{\boldsymbol{u}}]$ is calculated accurately.

Numerical examples

Scattering of an incident plane wave by a penny-shaped nonlinear interface crack with radius a, as shown in Fig. 3, is analyzed by the proposed method. The material constants are shown in Table 1

Table 1. Material constants

	c_L [m/s]	c_T [m/s]	ρ [kg/m^3]
D^I (steel)	5800	3100	7690
D^{II} (aluminum)	6400	3040	2700

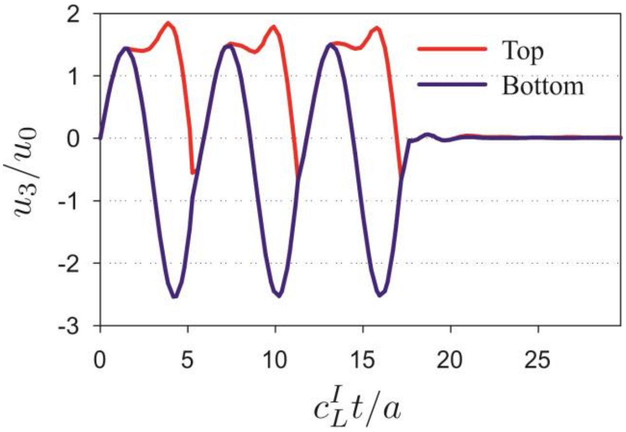

Figure 4. Vertical displacements at the center points on top and bottom surfaces of an interface crack of bi-material as a function of time.

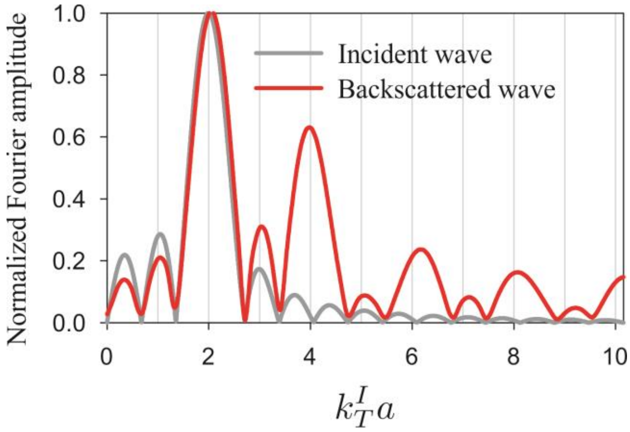

Figure 5. Normalized Fourier amplitudes of backscattered L wave at far-field and incident wave as a function of wave number.

and the static and dynamic friction coefficients, μ_s and μ_d, are given by $\mu_s = 0.61$ and $\mu_d = 0.47$, respectively. The incident plane wave is given by a three cycle sinusoidal wave with amplitude u_0.

Fig. 4 shows the vertical displacements at the center points on top and bottom surfaces of the interface crack subjected to the normal incident L wave with the normalized wave number $k_T^I a = 2\pi a f / c_T^I = 2.0$ where f is the center frequency of the incident wave. In Fig. 4, the clapping motion occurs at the crack face. The crack opening displacement rapidly decreases and then vanishes when the crack is completely closed. Fourier spectra of the backscattered far-field amplitude $\Omega_L/(a u_0)$ and the incident wave are shown in Fig. 5. These spectra are normalized by their maximum values. It is observed that large higher-harmonics components are included in the backscattered wave.

Conclusions

In this paper, the boundary integral formulation, interface conditions, and numerical algorithm for the simulation of an interface crack of bi-material subjected to an incident plane wave are presented. Moreover, the calculation method of far-field amplitude for the two-layer problem, and numerical results of normal incidence of L wave are shown. From the numerical results, the generation of higher-harmonics by CAN was confirmed using the proposed method. Additional numerical examples, such as oblique incidence, will be shown in near future.

References

Achenbach, J. D., Gautesen, A. K. and McMaken, H. (1982) Ray methods for waves in elastic solids, *Pitman*.

Buck, O., Morris, W. L. and Richardson, J.M. (1978) Acoustic harmonic generation at unbonded interfaces and fatigue cracks, *Applied Physics Letters* **33**, 371–373.

Hirose, S. and Achenbach, J. D. (1989) Time-domain boundary element analysis of elastic wave interaction with a crack, *International Journal for Numerical Methods in Engineering*, **28**, 628–644.

Hirose, S. and Achenbach, J. D. (1993) Higher harmonics in the far-field due to dynamic crack-face contacting, *Journal of the Acoustical Society of America*, **93**, 142–147.

Hirose, S. (1994) 2-D scattering by a crack with contact boundary conditions, *Wave Motion*, **19**, 37–49.

Lubich, C. and Ostermann A. (1993) Runge-Kutta methods for parabolic equations and convolution quadrature, *Mathematics of Computation*, **60**, 105-131.

Maruyama, T., Saitoh, T. and Hirose, S. (2013) Implicit Runge-Kutta based convolution quadrature time-domain fast multipole boundary element method for 3-D scalar wave problems, *Journal of JSCE Applied Mechanics*, **69**, I_175–I_185 (in Japanese).

Ohara, Y., Horinouchi, S., Hashimoto, M., Shintaku, Y. and Yamanaka, K. (2011) Nonlinear ultrasonic imaging method for closed cracks using subtraction of responses at different external loads, *Ultrasonics*, **51**, 661-666.

Saitoh, T., Furuta, Y., Hirose, S. and Nakahata, K. (2011) Simulation of higher harmonics on nonlinear ultrasonic testing using convolution quadrature time-domain boundary element method in 2-D elastodynamics, *Journal of JSCE Applied Mechanics*, **67**, I_161–I_169 (in Japanese).

Solodov, I., Doring, D. and Busse, G. (2011) New opportunities for NDT using non-linear interaction of elastic waves with defects, *Journal of Engineering Mechanics*, **57**, 169–182.